Supporting Information

for

Ultrasound Enhanced Adsorption of Chromium (VI) on Fe_3O_4 Magnetic Particles

[†] Department of Applied Chemistry, Anhui University of Technology, Maanshan, Anhui 243002, P. R. China

[‡] Analysis and Testing Central Facility, Anhui University of Technology, Maanshan, Anhui, 243002, P. R. China

Wang-Bing Zhang *[†], *Miao Deng* [†], *Chu-Xiao Sun* [†], *Shang-Bing Wang** [‡]

***Corresponding Author**

Tel: +86-555-2311807.

Fax: +86-555-2311822.

E-mail: zhangwb@ahut.edu.cn

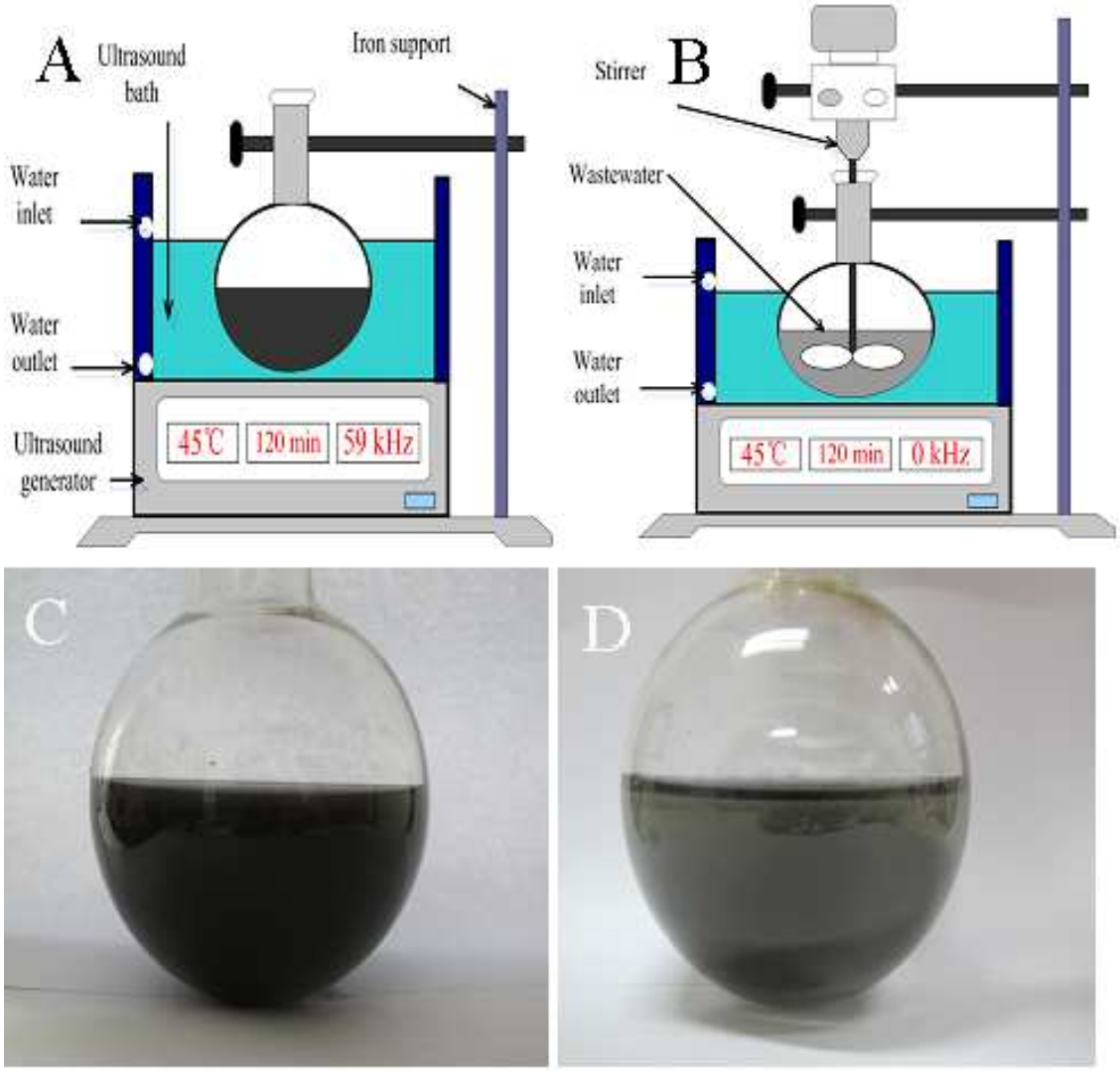

Figure S1. (A) and (B) Scheme of the experimental setup for sorption in presence of ultrasonic field and stirring mode; (C) and (D) Photograph of solution after ultrasound and stirring.

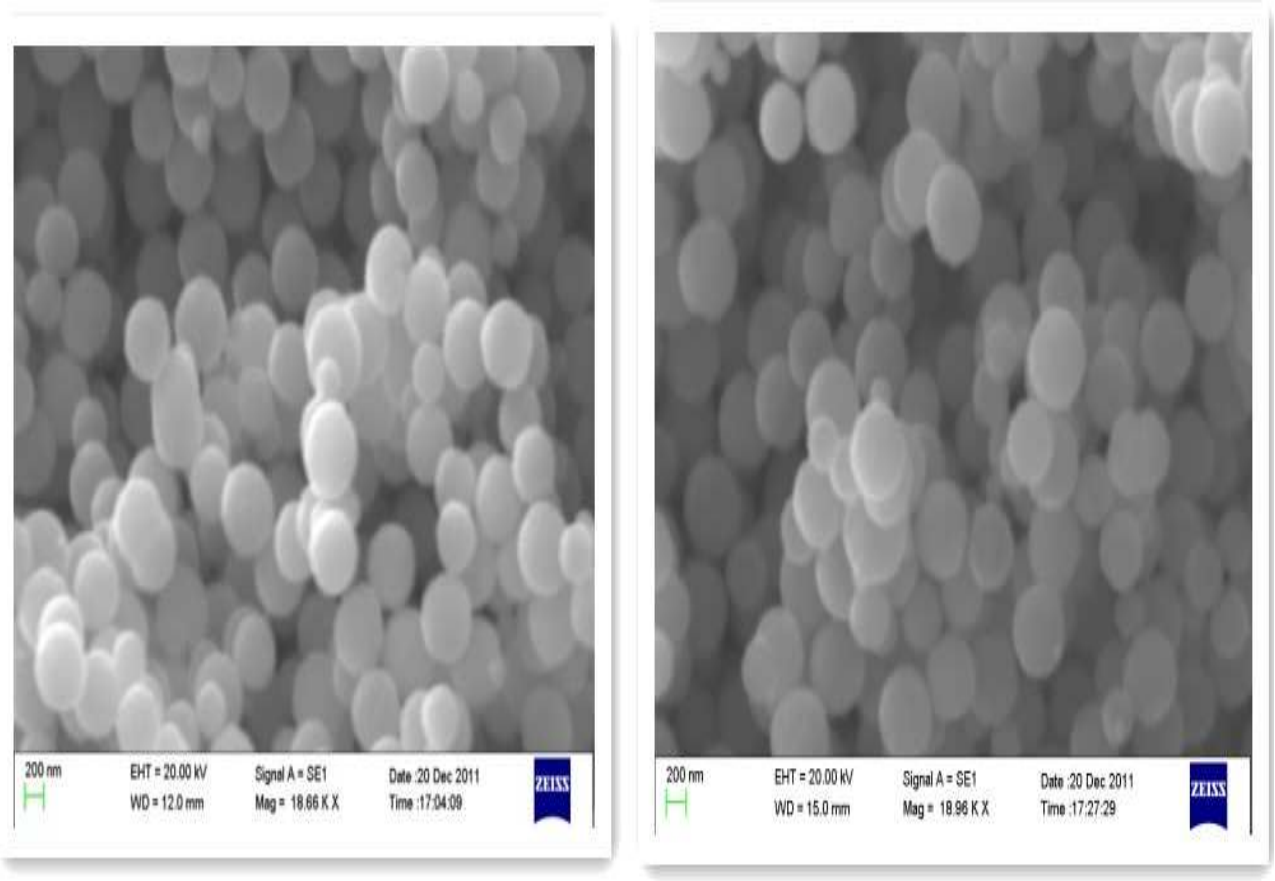

Figure S2. The SEM image of the as-prepared FMPs in the presence (left) and absence of ultrasound (right).

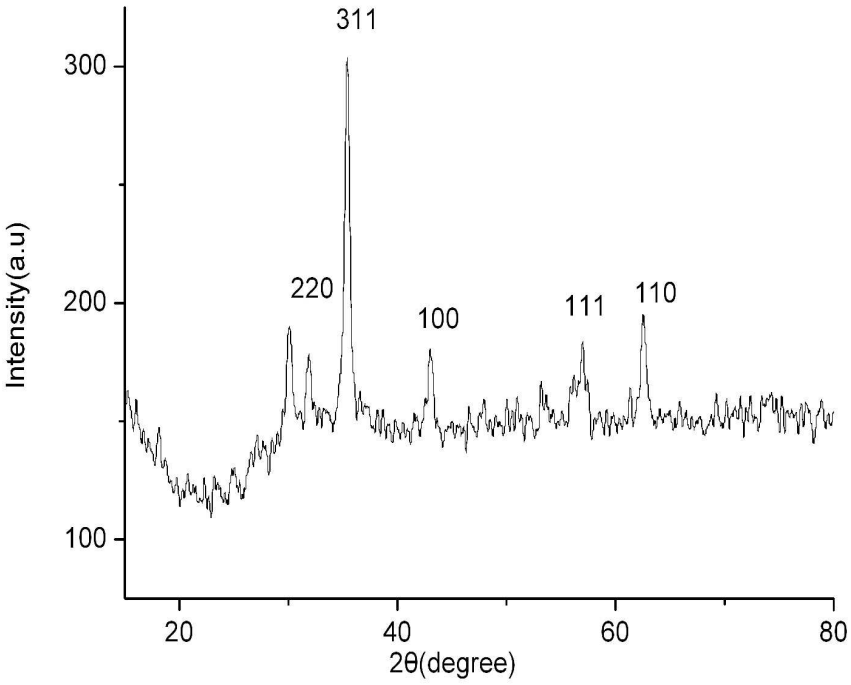

Fig S3. XRD patterns of Fe_3O_4

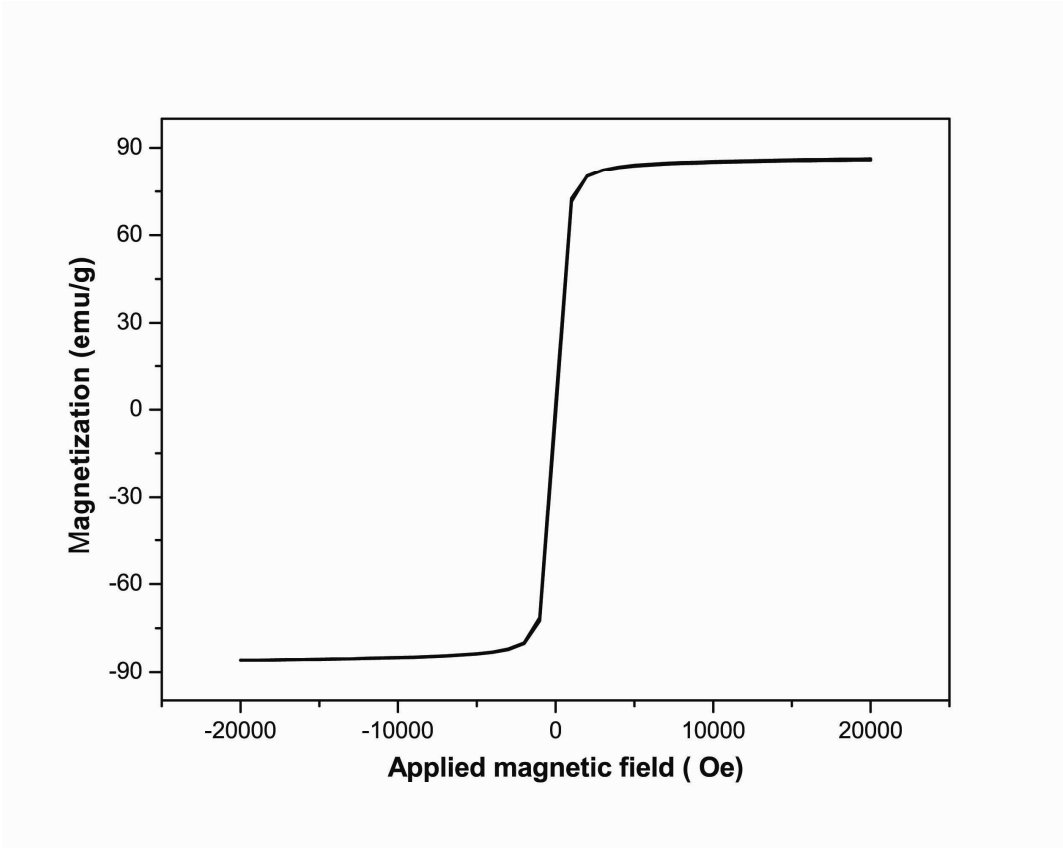

Figure S4. M-H curve of the Fe_3O_4 microspheres at 300K

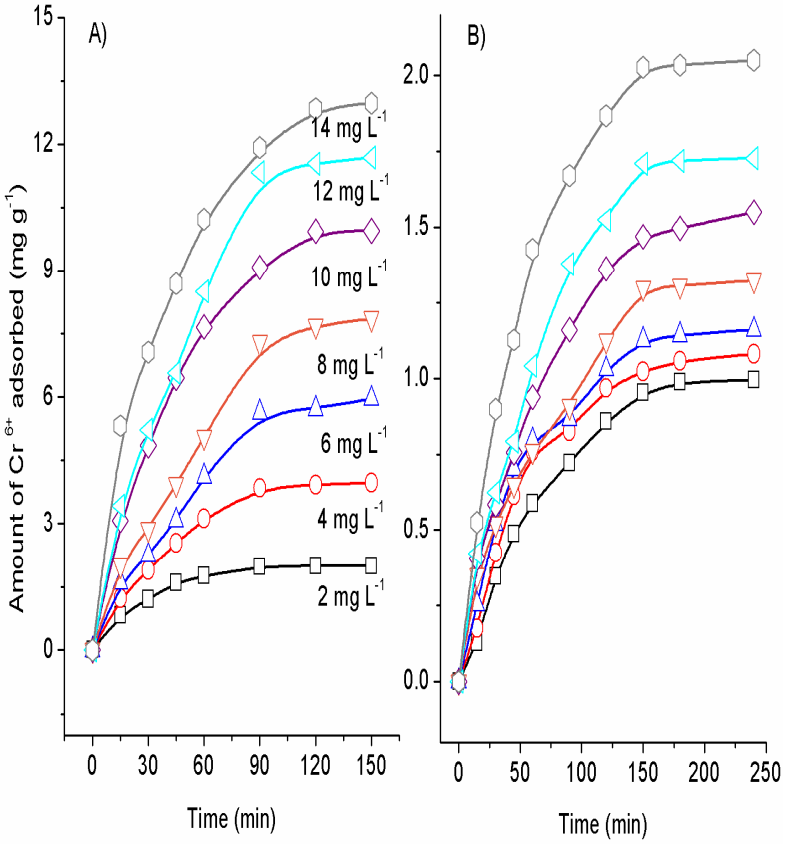

Figure S5. Effect of initial concentration on the sorption of Cr (VI): (A) for ultrasound mode (sorbent = 0.05 g, ultrasonic frequency = 59 kHz, ultrasonic power = 200 W, ultrasonic temperature = 318±2 K), (B) for stirring mode (sorbent = 0.05 g, temperature = 318±2 K).

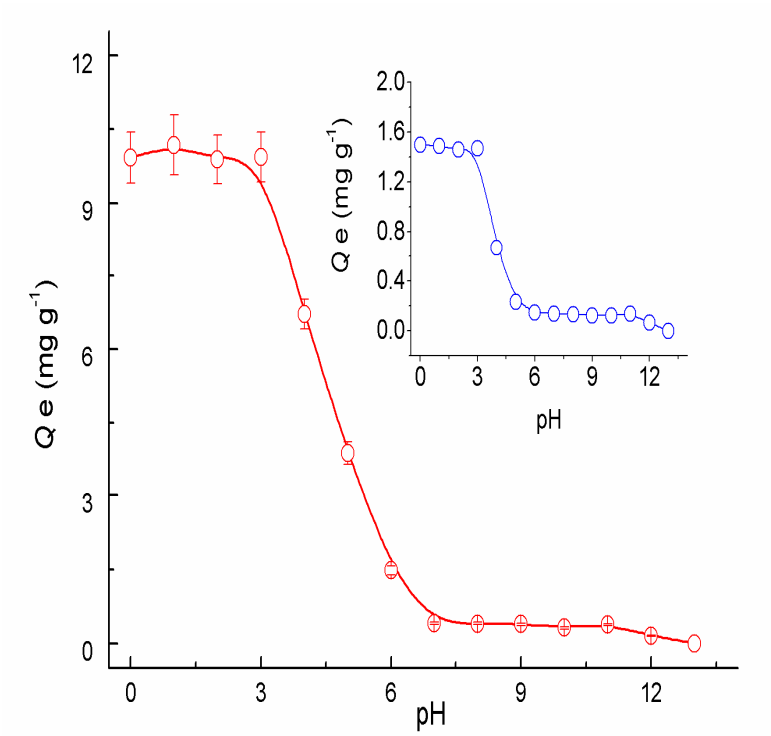

Figure S6. Effect of initial pH on the sorption of Cr (VI) for ultrasound mode (sorbent = 0.05 g, ultrasonic frequency = 59 kHz, ultrasonic power = 200 W, ultrasonic temperature = 318±2 K); insert images for stirring mode (sorbent = 0.05 g, temperature = 318±2 K).

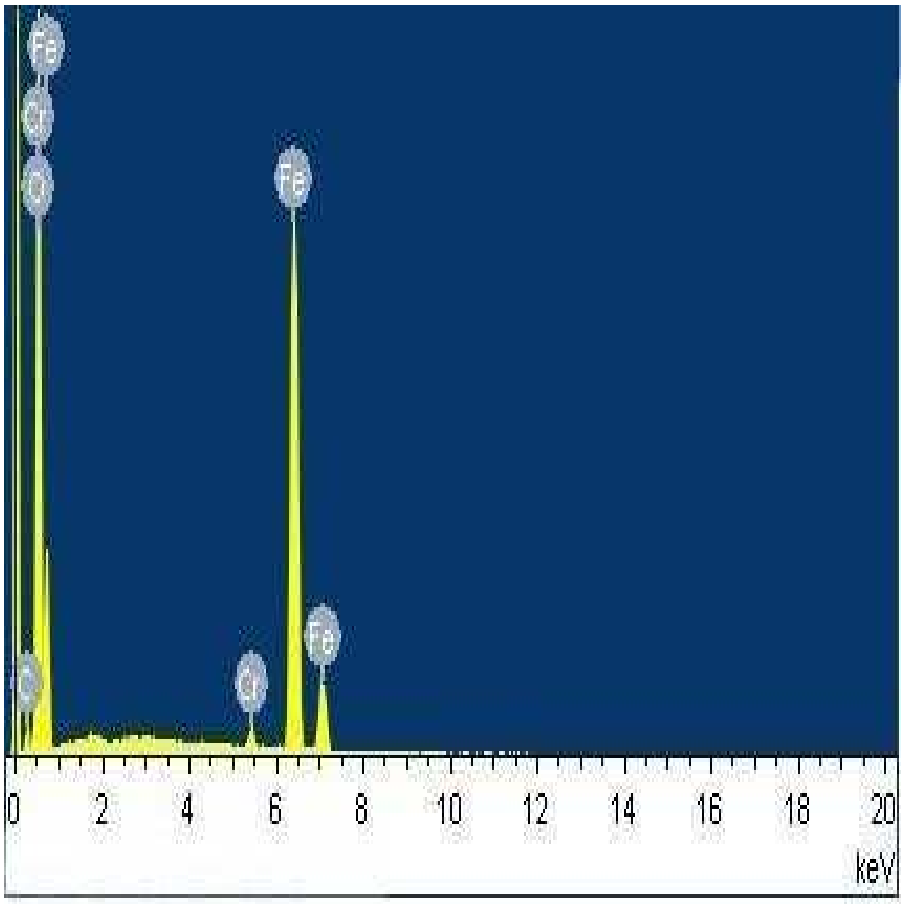

Figure S7. The energy-dispersive X-ray analysis of Cr (VI)-adsorbed FMPs.

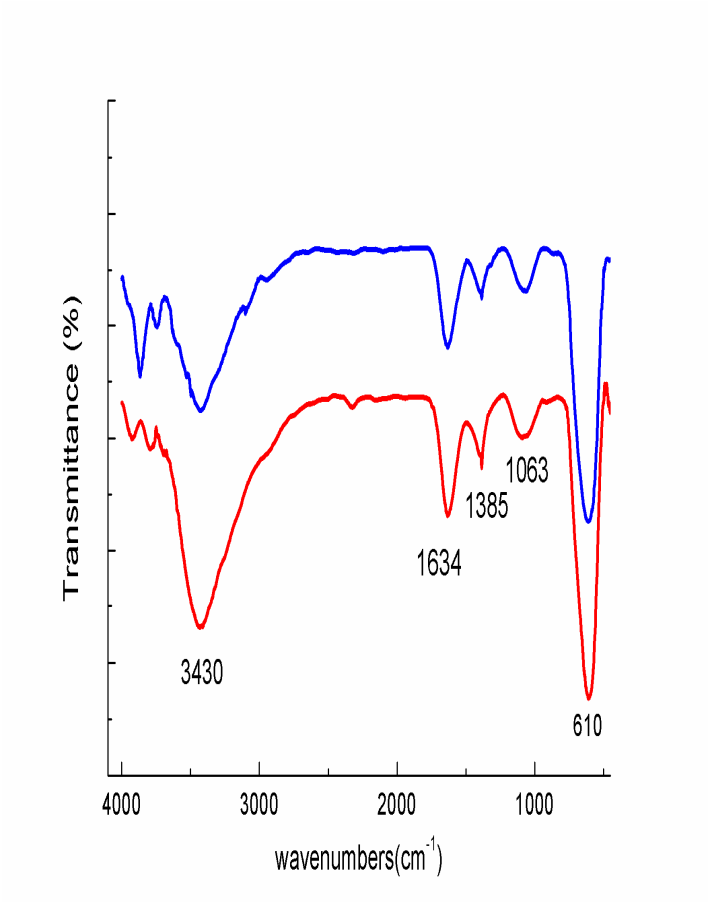

Figure S8. Infrared spectra of the as-prepared and Cr (VI)-adsorbed FMPs: red line and blue line are expressed as in presence and absence of ultrasound, respectively.

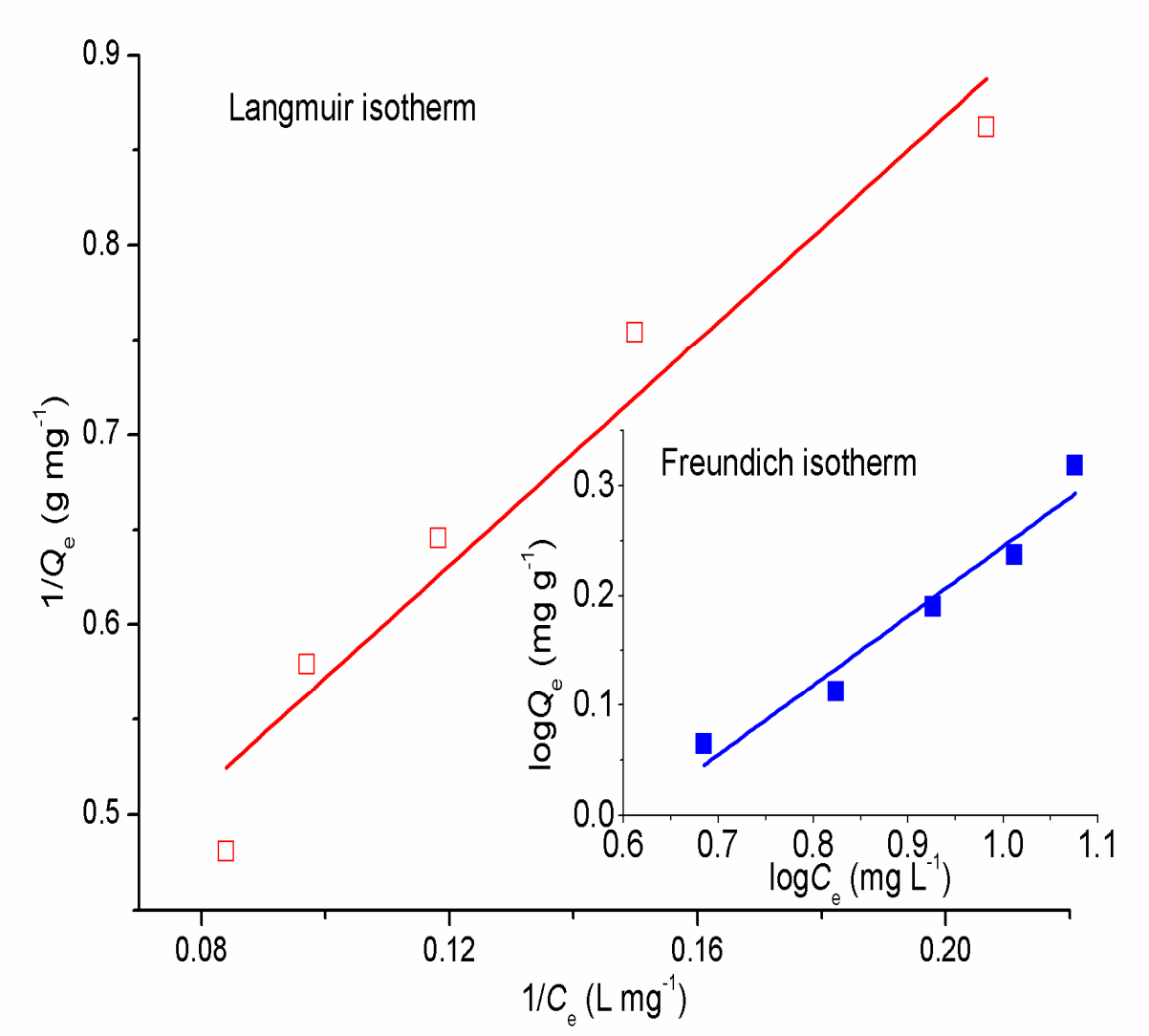

Figure S9. Adsorption isotherms for adsorption of Cr (VI) on FMNPs with stirring mode (sorbent = 0.05 g, temperature = 318±2 K).

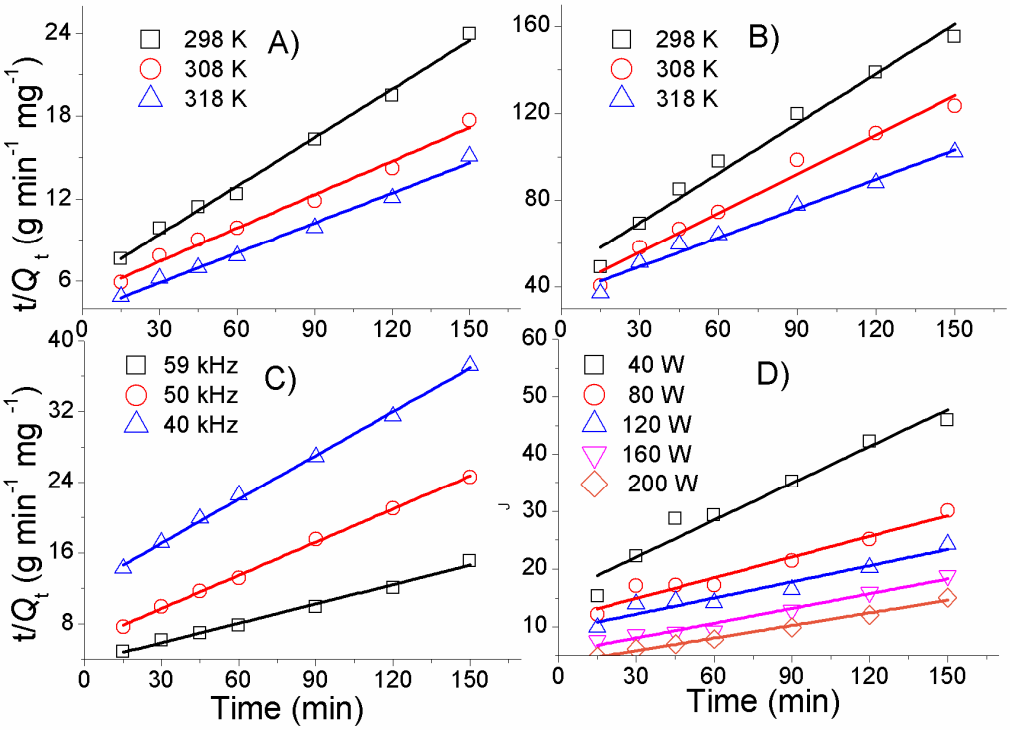

Figure S10. Pseudo-second-order kinetics model of Cr (VI): (A) and (B) are expressed as in presence and absence of ultrasound with different temperature, respectively; (C) and (D) for different frequency and power, respectively (1.0 g L^{-1} sorbent, pollutant = 10 mg L^{-1},).

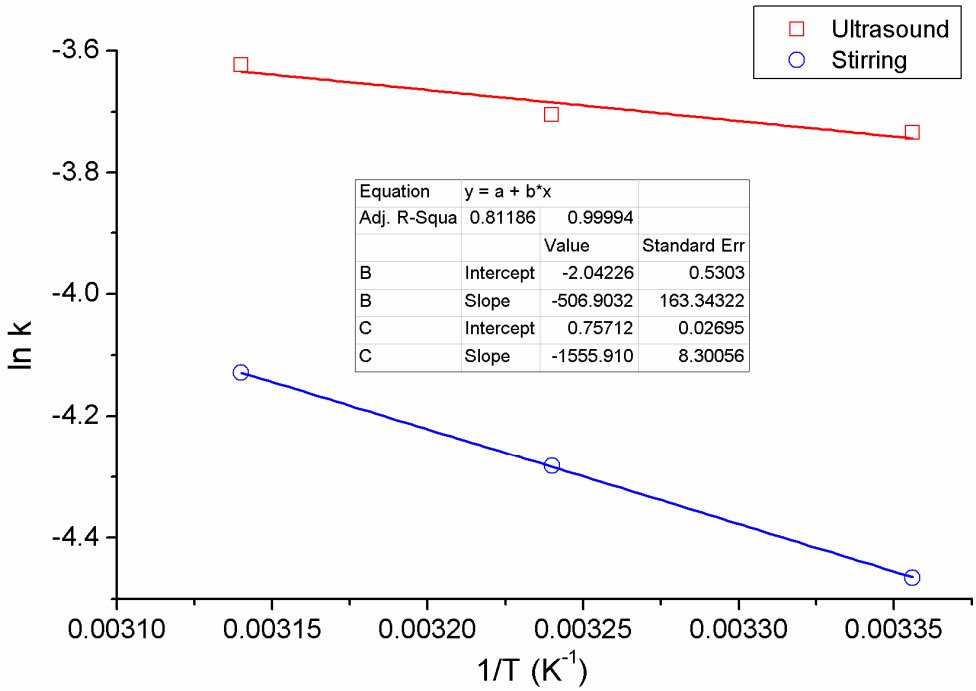

Figure S11. Logarithm of Pseudo-first-order rate constant versus 1/*T*: red line and blue line are expressed as in presence and absence of ultrasound, respectively.

Table S1 Adsorption parameters of pseudo-second-order obtained from the kietics for the adsorption Cr (VI) on FNPs with different temperature and ultrasonic frequency.

Mode	Temperature (K)	Frequency (k Hz)	Power (W)	k_2 (min^{-1})	$Q_{e\ (exp)}$ (mg g^{-1})	$Q_{e\ (catl)}$ (mg g^{-1})	R^2	h [a] (mg g^{-1} min^{-1})
Ultrasound	298	59	200	0.00233	6.25	8.53	0.994	0.1695
	308	59	200	0.00131	8.47	12.33	0.986	0.1992
	318	59	200	0.00143	9.95	13.76	0.990	0.2708
	318	50	200	0.00503	6.11	5.77	0.998	0.1675
	318	40	200	0.00498	4.03	4.07	0.998	0.0810
	318	59	40	0.00293	3.27	4.67	0.956	0.0639
	318	59	80	0.00126	4.98	8.38	0.951	0.0882
	318	59	120	0.00092	6.18	10.73	0.934	0.1063
	318	59	160	0.00132	7.96	11.72	0.962	0.1816
Stirring	298	/	/	0.0125	0.97	1.31	0.975	0.0215
	308	/	/	0.00953	1.22	1.66	0.977	0.0263
	318	/	/	0.00561	1.47	2.23	0.978	0.0279

[a]: the initial sorption rate h (mg g^{-1} min^{-1}) is calculated by the equation $h = k_2 Q_e^{\ 2}$

Table S2 Adsorption capacities of Cr (VI) on various sorbents

Sorbent	Capacity (mg g^{-1})	Reference
Riverbed sand	0.15	1
Coconut shell powder	1.23	2
Wollastonite	0.83	3
Fly ash	1.4	4
Actived alumina	1.6	5
Sawdust	3.6	6
Wheat bran	0.942	7
Spent activated clay	1.5	8
Metal layered double hydroxide	28	9
Aminated polyacrylonitile fiber	20.7	10
Magnetic nanoparticles*	3.56	11
Palygorskite clay	58.5	12
Fe_3O_4 magnetic particles	2.03 (Stirring) 12.30 (Ultrasound)	This work

References

(1) Sharma, Y. C.; Weng, C. H. Removal of chromium(VI) from water and wastewater by using riverbed sand: Kinetic and equilibrium studies. *J. Hazard. Mater.* **2006**, *142,* 449 –454.

(2) Pino, G. H.; Mesquita-De, L. M. S.; Torem, M. L.; Pinto, G. A. S. Biosorption of heavy metals by powder of green coconut shell. *Sep. Sci. Technol.* **2006**, *41,* 3141 –3153.

(3) Sharma,Y.C. Effect of temperature on interfacial adsorp-tion of Cr（VI) on wolla stonite. *J. Colloid Interface Sci.* **2001**, *233,* 265 – 270.

(4) Banarjee, S. S.; Joshi, M. V.; Jayaram, R. V. Removal of Cr(VI) and Hg(II) from aqueous solutions usingfl y ash and impregnated fly ash. *Sep. Sci. Technol.* **2004**, *39,* 1611 –1629

(5) Bishnoi, N. R.; Bajaj, M.; Sharma, N.; Gupta, A. Adsorption of Cr(VI) on activated rice husk carbon and activated alumina. *Bioresour. Technol.* **2004**, *91,* 305 –307.

(6) Baral, S. S.; Das, S. N.; Rath, P. Hexavalent chromium removal from aqueous solution by adsorption on treated sawdust. *Biochem. Eng. J.* **2006**, *31,* 216 –222.

(7) Nameni, M.; Moghadam, A. M. R.; Armani, M. Adsorption of hexavalent chromium from aqueous solutions by wheat bran. *Int. J. Environ. Sci. Technol.* **2008,** *5,* 161 –168.

(8) Weng, C. H.; Sharma, Y. C.; Chu, S. H. Adsorption of Cr(VI) from aqueous solutions by spent activated clay. *J. Hazard. Mater.* **2008,** *155,* 65–75.

(9) Das, N. N.; Konar, J.; Mohanta, M. K.; Srivastava, S. C. Adsorption of Cr(VI) and Se(IV) from their aqueous solutions onto Zr^{4+}-substituted ZnAl/MgAl-layered double hydroxides: effect of Zr^{4+} substitution in the layer. *J. Colloid Interface Sci.* **2004**, *270,* 1-8.

(10) Vermeulen, T. Theory for Irreversible and Constant-Pattern Solid Diffusion. *Ind. Eng. Chem.* **1953**, *45,* 1664-1670.

(11) Sharma. Y. C.; Srivastava. V. Comparative Studies of Removal of Cr (VI) and Ni(II) from Aqueous Solutions by Magnetic Nanoparticles. *J. Chem. Eng. Data.* **2011**, *56,* 819–825.

(12) Potgieter, J. H.; Potgieter-Vermaale, S. S.; Kalibantonga, P. D. Heavy metals removal from solution by palygorskite clay. *Miner. Eng.* **2006**, *19,* 463–470.